

# The Optical Gravitational Lensing Experiment. Eclipsing Binary Stars in the Large Magellanic Cloud\*

L. Wyrzykowski<sup>1</sup>, A. Udalski<sup>1</sup>, M. Kubiak<sup>1</sup>,  
M. Szymański<sup>1</sup>, K. Żebruń<sup>1</sup>, I. Soszyński<sup>1</sup>,  
P.R. Woźniak<sup>2</sup>, G. Pietrzyński<sup>1,3</sup> and  
O. Szewczyk<sup>1</sup>

<sup>1</sup> Warsaw University Observatory, Al. Ujazdowskie 4, 00-478 Warsaw, Poland  
e-mail:

(wyrzykow,udalski,mk,msz,zebrun,soszynsk,pietrzyn,szewczyk)@astrouw.edu.pl

<sup>2</sup> Princeton University Observatory, Princeton, NJ 08544-1001, USA  
Los Alamos National Observatory, MS-D436, Los Alamos NM 85745, USA  
email: wozniak@lanl.gov

<sup>3</sup> Universidad de Concepción, Departamento de Física, Casilla 160-C,  
Concepción, Chile  
email: pietrzyn@hubble.cfm.udec.cl

## ABSTRACT

We present the catalog of 2580 eclipsing binary stars detected in 4.6 square degree area of the central parts of the Large Magellanic Cloud. The photometric data were collected during the second phase of the OGLE microlensing search from 1997 to 2000. The eclipsing objects were selected with the automatic search algorithm based on an artificial neural network. Basic statistics of eclipsing stars are presented. Also, the list of 36 candidates of detached eclipsing binaries for spectroscopic study and for precise LMC distance determination is provided. The full catalog is accessible from the OGLE INTERNET archive.

*binaries: eclipsing – Magellanic Clouds – Catalogs*

## 1. Introduction

Eclipsing binary stars are among the most important sources of information on stellar parameters like radii, masses, luminosities, etc. They also seem to be very promising candidates for standard candles. They should allow to determine distances within the Local Group with accuracy of a few percent (Paczynski 1997). The method of distance determination to eclipsing systems is almost hundred years old and its main advantage is that it is largely geometric, *i.e.*, free from possible population effects which affect other standard candles. With accurate photometry and spectroscopy, absolute dimensions of both components can be precisely derived and, with accurately determined temperatures, emitted fluxes can be calculated. When compared with the flux observed from the Earth it should give precise distance to the binary.

---

\*Based on observations obtained with the 1.3 m Warsaw telescope at the Las Campanas Observatory of the Carnegie Institution of Washington.

Eclipsing binary stars are very common in the Universe, but their detection may be quite difficult, because very good sampling of the light curve is necessary to detect eclipses. Large photometric databases collected during microlensing surveys provide ideal observational material for search for eclipsing objects. Hundreds of observations of millions of stars make detection of eclipsing objects relatively easy and efficient. For example, large samples of eclipsing binary stars were already found in the Large Magellanic Cloud (Grison *et al.* 1995, Alcock *et al.* 1997), Small Magellanic Cloud (Udalski *et al.* 1998a) or Galactic bulge (Udalski *et al.* 1997a).

Determination of accurate distances is one of the most important goals of the modern astrophysics, in particular, the distance to the LMC as the extragalactic distance scale is based on the LMC distance. In the long lasting dispute on the LMC distance, large sample of eclipsing binary stars can potentially solve this problem. To date several applications of eclipsing binaries for distance determination to the LMC were presented: HV982 (Fitzpatrick *et al.* 2002), EROS1044 (Ribas *et al.* 2002). However single stars determination can be affected by all kind of systematic errors (*e.g.*, HV2274: Guinan *et al.* 1998, Udalski *et al.* 1998b, Nelson *et al.* 2000, Groenewegen and Salaris 2001). Large and consistent sample of eclipsing stars is necessary for obtaining reliable distances to objects, as it was shown in Harries *et al.* (2003), based on OGLE-II catalog of about 1400 eclipsing binaries in the SMC (Udalski *et al.* 1998a).

The main aim of this paper is to provide a list and photometry of eclipsing binary stars detected in the Large Magellanic Cloud during the OGLE-II survey (Udalski, Kubiak and Szymański 1997b). The catalog contains 2580 objects found in the Difference Image Analysis Catalog of variable stars in the LMC (Żebruń *et al.* 2001b).

The detected eclipsing binaries were divided into three classical types of eclipsing variables: EA (Algol type), EB ( $\beta$  Lyr type) and EW (W UMa type). The sample is reasonably complete, allowing statistical analysis and should provide a good material for testing theory of evolution of binary system as well as studying the LMC evolution, star formation etc. From detached systems, *i.e.*, EA class of eclipsing binaries, we additionally selected 36 objects – the best candidates for distance determination to the LMC. We also describe automated algorithm based on artificial neural network developed for eclipsing star search which can be applied in the future for other large scale variable stars' classifications.

## 2. Observational Data

All photometric data presented in the catalog of eclipsing stars were collected with the 1.3-m Warsaw telescope at the Las Campanas Observatory, Chile, which is operated by the Carnegie Institution of Washington, during the second phase of the OGLE experiment. The telescope was equipped with the “first generation” camera with the SITe 2048x2048 CCD detector working in driftscan mode. The pixel size was  $24\mu\text{m}$  giving the scale of 0.417 arcsec/pixel.

Observations of the LMC were performed in the “slow” reading mode of the CCD detector with the gain  $3.8\text{e}^-/\text{ADU}$  and readout noise of about  $5.4\text{ e}^-$ . Details of the instrumentation setup can be found in Udalski, Kubiak and Szymański (1997b).

Regular observations of the LMC fields started on January 6, 1997 and covered about 4.5 square degrees of the central parts of the LMC. Reductions of the photometric data collected up to the end of May 2000 were performed with the Difference Image Analysis (DIA) package (Woźniak 2000, Żebruń, Soszyński and Woźniak 2001a) and variable stars candidates were published in the Catalog of variable stars in the Magellanic Clouds (Żebruń *et al.* 2001b).

T a b l e 1  
Equatorial coordinates of the LMC fields

Field	RA (J2000)	DEC (J2000)
LMC_SC1	$5^{\text{h}}33^{\text{m}}49^{\text{s}}$	$-70^{\circ}06'10''$
LMC_SC2	$5^{\text{h}}31^{\text{m}}17^{\text{s}}$	$-69^{\circ}51'55''$
LMC_SC3	$5^{\text{h}}28^{\text{m}}48^{\text{s}}$	$-69^{\circ}51'55''$
LMC_SC4	$5^{\text{h}}26^{\text{m}}18^{\text{s}}$	$-69^{\circ}48'05''$
LMC_SC5	$5^{\text{h}}24^{\text{m}}48^{\text{s}}$	$-69^{\circ}41'05''$
LMC_SC6	$5^{\text{h}}21^{\text{m}}18^{\text{s}}$	$-69^{\circ}37'10''$
LMC_SC7	$5^{\text{h}}18^{\text{m}}48^{\text{s}}$	$-69^{\circ}24'10''$
LMC_SC8	$5^{\text{h}}16^{\text{m}}18^{\text{s}}$	$-69^{\circ}19'15''$
LMC_SC9	$5^{\text{h}}13^{\text{m}}48^{\text{s}}$	$-69^{\circ}14'05''$
LMC_SC10	$5^{\text{h}}11^{\text{m}}16^{\text{s}}$	$-69^{\circ}09'15''$
LMC_SC11	$5^{\text{h}}08^{\text{m}}41^{\text{s}}$	$-69^{\circ}10'05''$
LMC_SC12	$5^{\text{h}}06^{\text{m}}16^{\text{s}}$	$-69^{\circ}38'20''$
LMC_SC13	$5^{\text{h}}06^{\text{m}}14^{\text{s}}$	$-68^{\circ}43'30''$
LMC_SC14	$5^{\text{h}}03^{\text{m}}49^{\text{s}}$	$-69^{\circ}04'45''$
LMC_SC15	$5^{\text{h}}01^{\text{m}}17^{\text{s}}$	$-69^{\circ}04'45''$
LMC_SC16	$5^{\text{h}}36^{\text{m}}18^{\text{s}}$	$-70^{\circ}09'40''$
LMC_SC17	$5^{\text{h}}38^{\text{m}}48^{\text{s}}$	$-70^{\circ}16'45''$
LMC_SC18	$5^{\text{h}}41^{\text{m}}18^{\text{s}}$	$-70^{\circ}24'50''$
LMC_SC19	$5^{\text{h}}43^{\text{m}}48^{\text{s}}$	$-70^{\circ}34'45''$
LMC_SC20	$5^{\text{h}}46^{\text{m}}18^{\text{s}}$	$-70^{\circ}44'50''$
LMC_SC21	$5^{\text{h}}21^{\text{m}}14^{\text{s}}$	$-70^{\circ}33'20''$

The DIA photometry is based on the *I*-band observations. The catalog of variable stars contains about 53 000 stars in 21 fields of the LMC (Table 1). Each star has at least 300 photometric measurements. The magnitudes of stars were transformed to the standard system (Udalski *et al.* 2000). The errors of the measurements are about 0.005 mag for the brightest stars ( $I < 16$  mag) and grow to 0.08 mag at 19 mag and to 0.3 mag at 20.5 mag.

### 3. Search for Eclipsing Binary Stars

The most common method of classification of variable stars is based on visual inspection of light curves, but when the number of stars to be examined is growing to thousands, it becomes very inefficient. Until now several attempts have been made to create an automated periodic variables classification. First method is examination of two dimensional projections of a multidimensional parameter space. Such an approach was applied by *e.g.*, Ruciński (1993, 1997), Szymański, Kubiak, Udalski (2001), for contact binaries, Mizerski and Bejger (2001) for RR Lyr and W UMa stars, Udalski *et al.* (1999) for Cepheids. Expanded and improved versions of this method were also applied by all sky surveys, as ROTSE (Akerlof 2000) and ASAS (Pojmański 2002) to classify variables into several common variability types.

Another method applied in automated classifications includes neural networks and machine learning algorithms (*e.g.*, Woźniak *et al.* 2001). We attempted to use an artificial neural network as a main classification tool to find eclipsing binaries among OGLE-II variable stars in the LMC.

#### 3.1 Preparation of Photometric Data

We performed the search on about 53000 stars from 21 fields of the LMC, published in the OGLE-II catalog of variable stars (Żebruń *et al.* 2001b).

First, all stars from the DIA catalog were checked for all kind irregularities in the light curve. This step allowed us to reject most non-periodic variables from the database. Next, all stars left (about 36 000) were searched for periodicity using AoV algorithm (Schwarzenberg-Czerny 1989). Because photometric data span about 1500 days we searched for periodicities in the wide range of 0.1–500 days.

Before the main process of recognition of variability types was started, some additional preparation steps were performed. To use the neural network, we had to convert the light curves of all periodic stars in such a way that the differences between them were only caused by differences of variability type. The main problem was caused by the AoV algorithm which sometimes detects not the correct period,  $P$ , but  $2 \times P$  or  $P/2$ . Therefore we performed a Fourier decomposition of phased light curves and examined the ratio of the first two coefficients. We did not change detected period if the ratio indicated that the first harmonic dominates, and divided it by two in other cases. In this way we further processed all eclipsing variables phased with periods  $P/2$ , and all pulsating (sinusoidal and wide class of “saw shape” type) with their correct periods.

At the last stage before running the network recognition we found zero phase for each light curve and we mapped the light curve as a  $70 \times 15$  pixel image. Examples of the projection of light curves are shown in Fig. 1.

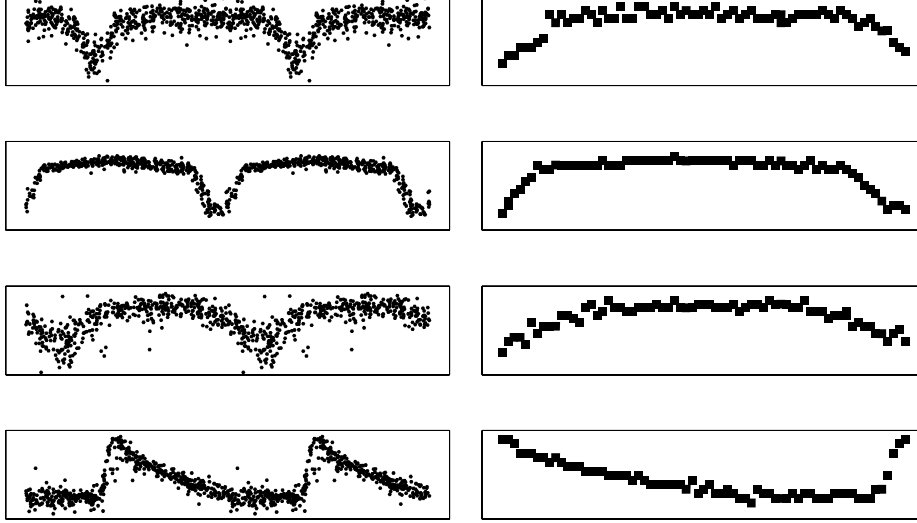


Fig. 1. Examples of conversion of phased light curves (*left*) to  $70 \times 15$  pixel images (*right*), which then entered the neural network. Notice that the light curves are shown twice (phases 0–2) for clarity, but the maps are shown only once, as they entered the network.

### 3.2 Neural Network

Now, the variability type recognition problem becomes the image recognition problem, which we solved using artificial neural network. Fig. 2 shows schematically the structure of the network. We built three layers, one-direction, non-linear neural network with logistic activation function. Input of the network was a  $70 \times 15$  pixel image of the light curve, which was transformed to one-dimensional line-by-line “image”. Therefore we had 1050 input nodes in the Input Layer. Layers I, II and III (Output Layer) consisted of 150, 50 and 5 neurons, respectively. Number of neurons in each layer was chosen accordingly to the image recognition requirements.

We used error back-propagation algorithm for network learning. Neural network was constructed to recognize three main types of variable stars, according to their light curve shape: eclipsing, sinusoidal and saw-shape type. From the first LMC field (LMC\_SC1) we selected manually 10 examples of each type objects and presented them randomly to the network a few thousand times, until the mean network error was smaller than  $10^{-8}$ .

After learning, light curves of all previously found periodical stars from all LMC fields were subject of the network analysis. The procedure allowed us to divide stars into main predefined types and exclude some artifacts and non-variable objects from the catalog. After this stage we could exclude the sinusoidal and saw-shaped variables and we were left with only about 3000 candidates for eclipsing variables.

fig2.jpg

Fig. 2. Schematic structure of artificial neural network used for automated search of eclipsing binary stars. Input layer has 1050 nodes, Layer I, II and Output Layer have 150, 50 and 5 neurons, respectively.

### 3.3 Detailed Classification of Eclipsing Variable Stars

In order to divide the obtained database of the eclipsing stars into subclasses we inspected visually light curves of all candidates. First, periods of eclipsing stars used in the network analysis were multiplied by two to obtain real periods. Then, the periods were tuned up to smooth the eclipse shape which is very sensitive to period inaccuracies. Similarly to the Fourth Edition of “General Catalog of Variable Stars” (GCVS: Kholopov *et al.* 1999) we divided detected eclipsing variables into three classical types, based on the shape of the light curve: EA (Algol type), EB ( $\beta$  Lyr type) and EW (W UMa type). For several stars dual classification (*e.g.*, EB/EW) was chosen, because of difficulties with distinguishing between two classes. The most difficult classification problem was the separation between EB and EW classes. When the orbital period was about one day or less we usually assigned EW type. In the case of several stars their variability, classification or period are uncertain. Such objects are marked with additional remark as “uncertain”.

By the visual inspection we excluded very uncertain objects and almost 200 light curves of probably ellipsoidal variables – stars with very low amplitude (about 0.1 mag) and in very wide range of periods. They were originally classified as eclipsing stars because the shape of their light curves revealed somewhat different depths of minima. The remaining part of ellipsoidal variables with clearly sinusoidal light curves were included in the “sinusoidal shape” class during neural network classification. However, in the case of some stars we were still unable to clearly distinguish between eclipsing and ellipsoidal variables. Therefore, they were also marked as ELL.

In the case of some objects additional variability of one or both components

was superimposed on the clear eclipsing variability. These light variations could be caused by *e.g.*, spots on binary system stars, high proper motion of the system (what is seen in the DIA method as a long term falling or rising tendency in the light curve, see Soszyński *et al.* 2002) or probably by pulsations of one of the binary components. The latter type systems containing Cepheids were already found in the LMC by OGLE (Udalski *et al.* 1999) and examined by MACHO Collaboration (Alcock *et al.* 2002). All variables with additional, confirmed or only suspected, light curve changes are marked with “Puls” or “Puls?” remark, respectively.

Additionally, we found 291 eclipsing variables with clear eccentricity effects visible in their light curves. They were marked with “ecc”. In 20 cases we could not smooth both eclipses using the same period what suggests large apsidal motion. We marked these objects as “eccAP” and selected the period corresponding to the primary minimum.

## 4. Catalog of Eclipsing Binary Stars

In total 2580 eclipsing binary stars were found in the OGLE-II DIA catalog of variable stars in the LMC fields. List of the first 50 stars is presented in Table 2. It contains the ordinal number of the eclipsing variable star, field, name of the star, orbital period, heliocentric Julian Date of the primary minimum ( $T_0 - 2\,450\,000$ , corrected for position of the star in the driftscan image, as described by Żebruń *et al.* 2001b),  $V$ -band magnitude,  $B - V$  and  $V - I$  colors at maximum brightness from the standard OGLE-II data pipeline photometry, amplitude in the  $I$ -band from DIA photometry (depth of primary minimum) and eclipsing type. Color value of  $-99.99$  stands for no observations in the  $B$  or  $V$  bands.

One should remember that the conversion of the DIA flux differences to the magnitude scale is not always accurate. In particular, in the case of severely blended objects the depth of the maxima can be unreliable, as the constant flux cannot be accurately determined. Nevertheless, such blends contain a real eclipsing star.

Among 2580 stars, 101 were identified twice in the overlapping regions between neighboring fields, so the total number of identified eclipsing binary stars is equal to 2681. List of all cross-identified objects is presented in Table 3.

Stars’ names follow the convention of Żebruń *et al.* (2001b), *i.e.*, are based on the equatorial coordinates of the star for the epoch J2000 in the format:

$$\text{OGLE}hhmmss.ss - ddmmss.s.$$

For example, OGLE053232.28-700056.5 stands for a star with coordinates  $\text{RA} = 05^{\text{h}}32^{\text{m}}32^{\text{s}}.28$  and  $\text{DEC} = -70^{\circ}00'56''.5$ .

1882 stars were classified as EA, 718 as EB and 168 as EW type. These figures do not sum up to 2681, because of several double classifications. Appendices A–C present examples of DIA  $I$ -band light curves of types EA, EB and EW, respectively. The ordinate is the phase with 0.0 value corresponding to the deeper eclipse. Abscissa is the  $I$ -band magnitude. Light curve is repeated twice for clarity.

Table 2  
Eclipsing binaries in the LMC

No.	Field	Star	Period [days]	$T_0$ −2450000	$V$	$B-V$	$V-I$	$\Delta I_{\text{PRI}}$ (DIA)	Type
1	LMC_SC1	OGLE053227.36-701148.4	1.843800	455.45870	19.16	−99.99	0.49	0.61	EB/EW
2	LMC_SC1	OGLE053230.79-700838.3	3.696430	455.45331	18.68	0.34	0.49	0.98	EA
3	LMC_SC1	OGLE053232.28-700056.5	1.225200	454.01971	17.69	−0.05	0.11	0.25	EB
4	LMC_SC1	OGLE053234.48-700218.2	1.577020	455.67840	18.33	0.06	0.17	0.44	EA
5	LMC_SC1	OGLE053235.27-702606.7	1.663420	456.09860	17.44	−0.04	0.05	0.19	EB
6	LMC_SC1	OGLE053236.25-700644.5	2.659240	457.37322	17.38	−0.16	0.11	0.22	EA
7	LMC_SC1	OGLE053236.80-695405.7	3.617860	452.71699	17.28	−0.07	−0.01	0.26	EA
8	LMC_SC1	OGLE053236.97-700317.1	1.849470	454.22510	19.01	−0.01	0.22	1.11	EB
9	LMC_SC1	OGLE053238.66-701354.2	5.481640	455.44523	17.47	−0.08	−0.05	0.27	EA
10	LMC_SC1	OGLE053240.31-701127.8	1.905630	456.59061	18.46	−0.04	0.25	1.45	EA
11	LMC_SC1	OGLE053241.43-694149.3	136.423800	491.06174	18.55	1.04	1.19	0.15	EA
12	LMC_SC1	OGLE053241.93-695109.2	4.954340	453.59493	16.87	−0.12	−0.04	0.54	EA
13	LMC_SC1	OGLE053242.83-700513.5	0.958740	455.71161	18.19	−0.31	0.40	0.31	EA
14	LMC_SC1	OGLE053244.07-695406.8	2.314920	455.76774	19.02	0.06	0.39	0.47	EA
15	LMC_SC1	OGLE053244.79-701621.5	3.047280	452.04025	19.92	−99.99	0.78	1.31	EA
16	LMC_SC1	OGLE053247.54-694403.1	0.331035	454.77797	17.34	0.63	0.89	0.42	EW
17	LMC_SC1	OGLE053248.27-703013.0	1.115930	455.09168	19.01	0.03	0.17	0.73	EA
18	LMC_SC1	OGLE053249.77-695445.5	5.749730	454.60472	16.94	0.00	0.08	0.69	EA
19	LMC_SC1	OGLE053251.37-701446.9	6.162960	450.94134	19.04	0.12	0.49	0.79	EA
20	LMC_SC1	OGLE053251.73-700256.2	0.297175	454.67085	17.71	0.86	0.98	0.77	EW
21	LMC_SC1	OGLE053252.71-694837.6	6.964140	454.61819	19.41	1.05	1.01	0.23	EA
22	LMC_SC1	OGLE053255.08-695837.9	0.901480	455.28013	18.86	0.19	0.22	0.65	EA
23	LMC_SC1	OGLE053257.90-700658.5	1.289960	456.12106	18.84	0.14	0.25	0.64	EA
24	LMC_SC1	OGLE053259.41-701152.3	5.738280	451.11831	19.59	0.24	0.61	1.59	EA
25	LMC_SC1	OGLE053259.97-695638.6	3.368120	456.82108	17.41	−0.02	0.10	1.59	EA
26	LMC_SC1	OGLE053300.70-701934.1	1.959150	455.52318	18.72	0.15	0.29	0.95	EA
27	LMC_SC1	OGLE053301.16-700805.4	3.340010	451.84411	19.45	0.65	0.76	0.59	EB
28	LMC_SC1	OGLE053302.18-700237.1	2.940790	457.21649	18.80	0.41	0.13	0.82	EA
29	LMC_SC1	OGLE053303.00-700516.8	1.115260	455.67346	18.69	−0.08	0.02	0.83	EA
30	LMC_SC1	OGLE053304.23-701613.1	69.773770	441.26483	17.79	0.79	0.94	0.16	EA
31	LMC_SC1	OGLE053306.15-695252.0	5.487330	457.61490	19.85	0.22	0.61	1.54	EA
32	LMC_SC1	OGLE053308.15-700112.0	0.877760	456.16928	18.58	0.07	0.11	0.61	EB
33	LMC_SC1	OGLE053308.85-695150.3	1.313040	454.49957	19.46	0.13	0.33	1.46	EA
34	LMC_SC1	OGLE053310.22-694618.9	26.451300	457.80026	18.88	0.89	1.09	0.43	EB
35	LMC_SC1	OGLE053311.25-702135.3	5.225480	455.47968	19.79	0.39	0.42	1.56	EA
36	LMC_SC1	OGLE053311.63-694400.2	2.144280	456.27341	18.65	0.01	0.04	0.67	EA-ecc
37	LMC_SC1	OGLE053311.89-694655.0	6.194370	452.65093	19.52	0.10	0.48	1.47	EA
38	LMC_SC1	OGLE053312.11-701124.8	7.937130	459.10728	18.56	0.13	0.18	0.59	EA
39	LMC_SC1	OGLE053312.82-700702.5	5.394410	454.74615	17.18	−0.06	−0.02	0.38	EA
40	LMC_SC1	OGLE053314.45-701708.8	2.580720	453.36055	18.46	−0.04	0.09	0.80	EA
41	LMC_SC1	OGLE053314.63-701005.3	1.795680	456.15587	16.94	0.31	0.04	0.18	EB/EW/ELL
42	LMC_SC1	OGLE053317.37-695605.2	23.913340	443.18485	19.47	0.89	1.41	1.02	EA
43	LMC_SC1	OGLE053318.69-695502.6	4.637010	452.73410	16.17	−0.02	0.01	0.90	EB
44	LMC_SC1	OGLE053320.14-702025.0	53.051330	525.69769	18.71	0.88	1.14	3.55	EA
45	LMC_SC1	OGLE053320.76-695427.7	1.559150	456.41948	17.57	−0.12	0.02	0.59	EA
46	LMC_SC1	OGLE053321.09-701743.3	6.108740	457.02623	19.52	0.64	1.17	0.65	EA
47	LMC_SC1	OGLE053323.38-700802.3	7.187350	456.73297	16.94	0.00	0.16	0.80	EA
48	LMC_SC1	OGLE053326.25-703114.1	2.945830	455.34469	17.53	−0.05	0.10	0.43	EA
49	LMC_SC1	OGLE053326.64-694404.2	3.546780	454.60046	19.63	0.26	0.55	1.18	EA
50	LMC_SC1	OGLE053327.35-695205.5	4.654350	451.62319	19.86	0.25	0.87	1.37	EA



Table 3

Cross-identification of eclipsing binary stars detected in overlapping regions

LMC_SC1 ↔ LMC_SC16	OGLE053458.41-701653.3	LMC_SC1 ↔ LMC_SC16	OGLE053459.53-694406.2
LMC_SC1 ↔ LMC_SC16	OGLE053500.64-701843.0	LMC_SC1 ↔ LMC_SC16	OGLE053502.18-694417.8
LMC_SC1 ↔ LMC_SC16	OGLE053504.85-695812.0	LMC_SC1 ↔ LMC_SC16	OGLE053509.05-700659.9
LMC_SC1 ↔ LMC_SC16	OGLE053509.40-694631.1	LMC_SC1 ↔ LMC_SC16	OGLE053512.36-702808.5
LMC_SC1 ↔ LMC_SC2	OGLE053227.36-701148.4	LMC_SC1 ↔ LMC_SC2	OGLE053230.79-700838.3
LMC_SC1 ↔ LMC_SC2	OGLE053234.48-700218.2	LMC_SC1 ↔ LMC_SC2	OGLE053236.80-695405.7
LMC_SC1 ↔ LMC_SC2	OGLE053236.97-700317.1	LMC_SC1 ↔ LMC_SC2	OGLE053238.66-701354.2
LMC_SC2 ↔ LMC_SC3	OGLE052956.44-694220.9	LMC_SC2 ↔ LMC_SC3	OGLE052957.18-701054.0
LMC_SC2 ↔ LMC_SC3	OGLE052957.34-695520.8	LMC_SC2 ↔ LMC_SC3	OGLE052958.05-701224.3
LMC_SC2 ↔ LMC_SC3	OGLE052958.13-695936.2	LMC_SC2 ↔ LMC_SC3	OGLE052958.54-695708.0
LMC_SC2 ↔ LMC_SC3	OGLE052959.80-694358.8	LMC_SC2 ↔ LMC_SC3	OGLE052959.87-695950.1
LMC_SC2 ↔ LMC_SC3	OGLE052959.88-695918.6	LMC_SC2 ↔ LMC_SC3	OGLE053000.05-695214.0
LMC_SC2 ↔ LMC_SC3	OGLE053001.64-693057.2	LMC_SC2 ↔ LMC_SC3	OGLE053002.59-700945.8
LMC_SC2 ↔ LMC_SC3	OGLE053005.04-692750.0	LMC_SC2 ↔ LMC_SC3	OGLE053005.21-694527.1
LMC_SC2 ↔ LMC_SC3	OGLE053006.98-695309.6	LMC_SC2 ↔ LMC_SC3	OGLE053007.56-695321.3
LMC_SC3 ↔ LMC_SC4	OGLE052726.58-700720.2	LMC_SC3 ↔ LMC_SC4	OGLE052728.35-694902.1
LMC_SC3 ↔ LMC_SC4	OGLE052728.57-694457.5	LMC_SC3 ↔ LMC_SC4	OGLE052729.79-695936.0
LMC_SC3 ↔ LMC_SC4	OGLE052730.73-695244.0	LMC_SC3 ↔ LMC_SC4	OGLE052736.26-693754.1
LMC_SC3 ↔ LMC_SC4	OGLE052737.48-692053.5	LMC_SC4 ↔ LMC_SC5	OGLE052456.31-700250.4
LMC_SC4 ↔ LMC_SC5	OGLE052456.76-694324.9	LMC_SC4 ↔ LMC_SC5	OGLE052456.78-694130.5
LMC_SC4 ↔ LMC_SC5	OGLE052458.44-693855.5	LMC_SC4 ↔ LMC_SC5	OGLE052459.33-692607.2
LMC_SC4 ↔ LMC_SC5	OGLE052500.95-693616.2	LMC_SC4 ↔ LMC_SC5	OGLE052501.42-695508.7
LMC_SC4 ↔ LMC_SC5	OGLE052501.51-700810.2	LMC_SC4 ↔ LMC_SC5	OGLE052503.58-694030.2
LMC_SC4 ↔ LMC_SC5	OGLE052503.66-692849.5	LMC_SC4 ↔ LMC_SC5	OGLE052503.68-692326.8
LMC_SC4 ↔ LMC_SC5	OGLE052504.39-695909.7	LMC_SC4 ↔ LMC_SC5	OGLE052504.94-694849.3
LMC_SC4 ↔ LMC_SC5	OGLE052506.70-695640.8	LMC_SC4 ↔ LMC_SC5	OGLE052509.46-700422.6
LMC_SC5 ↔ LMC_SC6	OGLE052229.91-691909.0	LMC_SC5 ↔ LMC_SC6	OGLE052230.88-694409.1
LMC_SC5 ↔ LMC_SC6	OGLE052233.86-693256.4	LMC_SC5 ↔ LMC_SC6	OGLE052235.40-693649.2
LMC_SC5 ↔ LMC_SC6	OGLE052235.87-695257.9	LMC_SC5 ↔ LMC_SC6	OGLE052236.06-694026.6
LMC_SC6 ↔ LMC_SC7	OGLE051958.16-692823.9	LMC_SC6 ↔ LMC_SC7	OGLE051959.79-692201.9
LMC_SC6 ↔ LMC_SC7	OGLE052002.15-692007.0	LMC_SC6 ↔ LMC_SC7	OGLE052003.88-692616.1
LMC_SC6 ↔ LMC_SC7	OGLE052007.03-692925.6	LMC_SC6 ↔ LMC_SC7	OGLE052008.00-693241.4
LMC_SC7 ↔ LMC_SC8	OGLE051729.24-692809.7	LMC_SC7 ↔ LMC_SC8	OGLE051734.42-694422.2
LMC_SC7 ↔ LMC_SC8	OGLE051734.54-692736.5	LMC_SC7 ↔ LMC_SC8	OGLE051736.06-693846.9
LMC_SC7 ↔ LMC_SC8	OGLE051737.60-693139.8	LMC_SC8 ↔ LMC_SC9	OGLE051500.27-691126.5
LMC_SC8 ↔ LMC_SC9	OGLE051502.03-691918.0	LMC_SC8 ↔ LMC_SC9	OGLE051502.88-690816.7
LMC_SC8 ↔ LMC_SC9	OGLE051506.39-693434.1	LMC_SC10 ↔ LMC_SC9	OGLE051230.07-690624.2
LMC_SC10 ↔ LMC_SC9	OGLE051232.66-685637.9	LMC_SC11 ↔ LMC_SC12	OGLE050726.38-693245.7
LMC_SC11 ↔ LMC_SC12	OGLE050728.63-692539.6	LMC_SC11 ↔ LMC_SC12	OGLE050730.20-693638.8
LMC_SC11 ↔ LMC_SC12	OGLE050731.85-691010.9	LMC_SC11 ↔ LMC_SC13	OGLE050731.61-690926.9
LMC_SC12 ↔ LMC_SC13	OGLE050511.63-691012.4	LMC_SC12 ↔ LMC_SC13	OGLE050609.82-691109.9
LMC_SC12 ↔ LMC_SC13	OGLE050638.95-691026.0	LMC_SC12 ↔ LMC_SC13	OGLE050659.47-691050.0
LMC_SC12 ↔ LMC_SC13	OGLE050712.75-691100.3	LMC_SC13 ↔ LMC_SC14	OGLE050503.92-685221.0
LMC_SC13 ↔ LMC_SC14	OGLE050504.24-685758.9	LMC_SC13 ↔ LMC_SC14	OGLE050504.90-690554.1
LMC_SC14 ↔ LMC_SC15	OGLE050234.59-690546.0	LMC_SC16 ↔ LMC_SC17	OGLE053726.41-702422.8
LMC_SC16 ↔ LMC_SC17	OGLE053734.07-701253.7	LMC_SC16 ↔ LMC_SC17	OGLE053734.55-694954.5
LMC_SC16 ↔ LMC_SC17	OGLE053738.73-700112.9	LMC_SC17 ↔ LMC_SC18	OGLE054003.85-703837.3
LMC_SC17 ↔ LMC_SC18	OGLE054008.14-701202.8	LMC_SC17 ↔ LMC_SC18	OGLE054008.22-700359.2
LMC_SC17 ↔ LMC_SC18	OGLE054009.08-703718.2	LMC_SC17 ↔ LMC_SC18	OGLE054010.85-703013.4
LMC_SC18 ↔ LMC_SC19	OGLE054229.84-701154.9	LMC_SC19 ↔ LMC_SC20	OGLE054509.85-703644.7
LMC_SC21 ↔ LMC_SC5	OGLE052230.33-700651.6		

Tables, light curves and finding charts of all 2681 eclipsing binary objects are available from the OGLE INTERNET archive and *via* the WWW Interface (Section 8).

We should stress that periods of several stars might be incorrect. First, period can be two times longer than the real one, because in some cases, the secondary eclipse of faint stars and for noisy light curves could not be reliably detected. Other possible period error, which was noticed during the visual inspection of light curves, was related with the AoV method. For stars with large eccentricity it triggered periods of  $1.5 \times P$  or  $2.5 \times P$  instead of the correct period  $P$ . We probably corrected most of such cases, but we cannot fully exclude that some of them are still in the catalog.

## 5. Discussion

We present 2580 eclipsing binary stars located in the central regions of the LMC. It is the largest number of eclipsing stars ever discovered in the LMC. We did not attempt to identify the detected stars with previously discovered eclipsing binaries in the LMC, but it is obvious, that the vast majority of these objects are newly discovered systems, because other published catalogs contain only 79 (EROS: Grison *et al.* 1995) and 611 (MACHO: Alcock *et al.* 1997) objects.

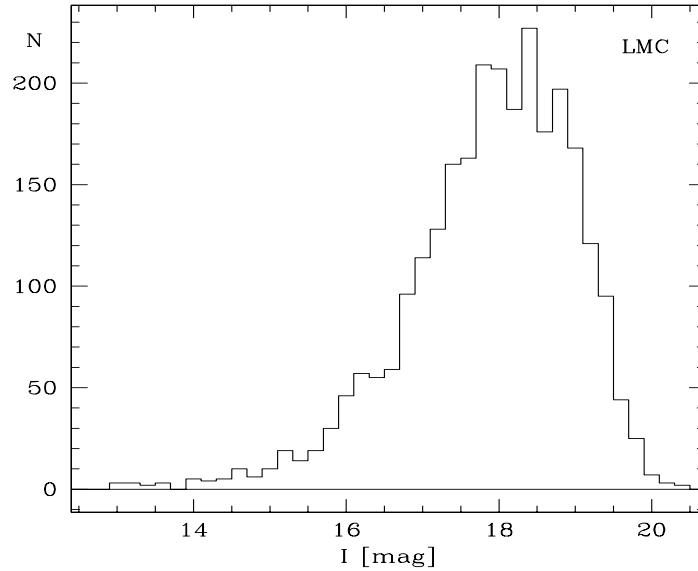


Fig. 3. Histogram of the DIA *I*-band brightness for eclipsing stars in 0.2 mag bins.

Very good quality of the DIA photometry is clearly visible in the light curves of presented stars. Also magnitude limit is low, as shown in Fig. 3, which presents the histogram of the DIA *I*-band brightness for all eclipsing stars found in the LMC.

fig4.jpg

Fig. 4. OGLE-II fields in the LMC. Dots indicate positions of eclipsing stars. North is up and East to the left in the DSS image.

Fig. 4 presents a picture of the LMC from the Digitized Sky Survey (DSS) with contours of the OGLE-II fields. Positions of the eclipsing binary stars are marked with black dots. The stars are distributed proportionally to the density of the LMC stars, with the largest concentration in the fields LMC\_SC2–LMC\_SC7.

Fig. 5 shows the histogram of orbital periods of the LMC eclipsing variables in 0.25 day bins from 0 to 10 days. Dashed, dot-dashed and solid lines correspond to classes EA, EB and EW, respectively and dotted line corresponds to all eclipsing objects. Additional 416 objects with periods longer than 10 days are distributed more or less uniformly and their number falls rapidly to zero at longer periods. The longest reliable period found among all objects equals to 251.096 days (LMC\_SC16 OGLE053725.90-700223.3), but there are two objects (LMC\_SC21 OGLE052052.41-700655.1 and LMC\_SC19 OGLE054310.48-703057.8), with only one or two eclipses observed, which periods can be even longer. However, these periods cannot be derived reliably with the present dataset.

The majority of stars are short period systems with the most frequent period of about 1.5 days. EA type is the most numerous class of eclipsing objects in the

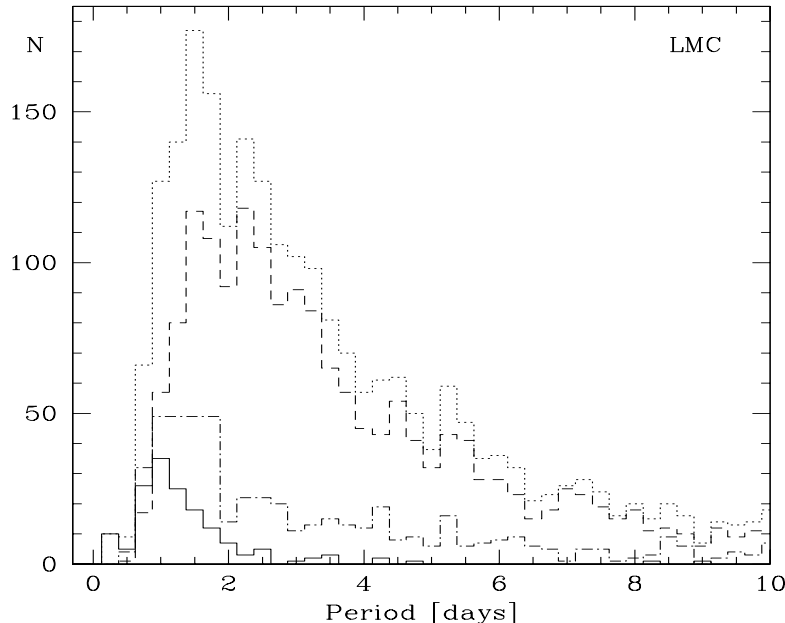


Fig. 5. Histogram of periods of eclipsing binaries in 0.25 day bins. Dashed, dot-dashed and solid lines correspond to classes EA, EB and EW respectively. Dotted line corresponds to all eclipsing objects. Additional 416 objects have periods longer than 10 days.

LMC. Its period distribution is characterized by a broad maximum at 1.5–2.5 days. Periods of stars from EB class are distributed with wide, flat maximum in the range of 1–2 days. The EW class is least numerous and has a maximum at periods of about 1 day. Distribution of the latter class is, however, severely biased because only long period tail of these objects from the LMC is bright enough to be in the range of the OGLE data. The remaining part of this class are foreground Galactic variables.

Fig. 6. presents  $I$  vs.  $V - I$  color-magnitude diagram for all eclipsing binary stars from the catalog. EA, EB and EW classes are marked with different symbols. Fig. 6 indicates, that almost all eclipsing stars belong to the LMC and there are only a few foreground systems. All three classes seem to be distributed uniformly over the CMD diagram.

In Fig. 7 we present CMD diagram for all eclipsing binary stars in the LMC, dividing stars into 4 groups depending on their periods: short, medium, long and very long. Each group is marked with different symbol. This plot was created similarly to the one for the eclipsing binaries found in the SMC (Fig. 3 in Udalski *et al.* 1998a). Both figures indicate close similarities in the distribution in the CMD of the eclipsing binary stars from both Magellanic Clouds. The majority of short and medium period eclipsing stars belong to the young population located on the main sequence. Long period stars are located in the lower giant branch

fig6.jpg

Fig. 6. Color-magnitude diagram of eclipsing binaries in the LMC. Solid dots, crosses and triangles mark EA, EB and EW type objects, respectively.

or on the right part of the main sequence, *i.e.*, they are probably evolved main sequence stars. Very long period stars are mostly concentrated in the upper part of the red giant branch.

## 6. Completeness of the Catalog and Network Efficiency

Assessment of the completeness of our catalog is important for statistical studies of eclipsing binaries in the LMC. Fig. 3, showing distribution of magnitudes of eclipsing objects, suggests that our sample should be complete to about  $I \approx 17.5$  mag. In general, the completeness is a function of magnitude, quality of photometry, period and other factors. We attempted to determine the mean completeness of our catalog by comparing objects detected in the overlapping regions of neighboring fields. Based on astrometric solutions, we checked, which of the de-

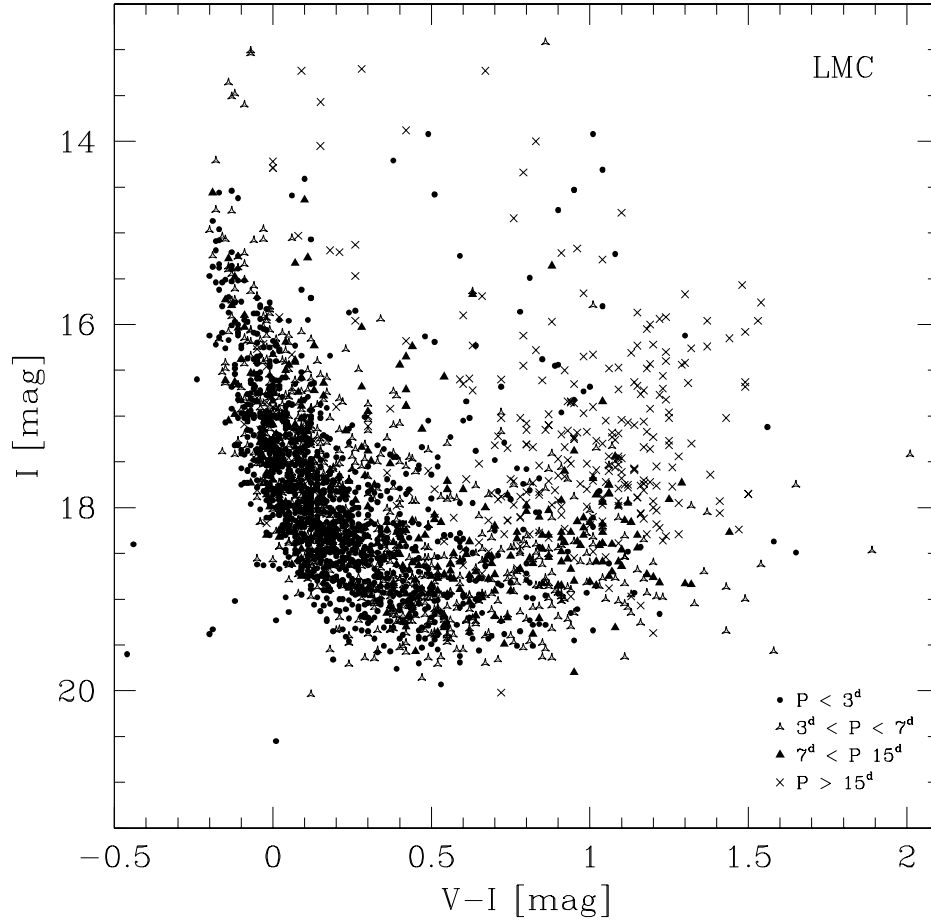


Fig. 7. Color-magnitude diagram of eclipsing binaries in the LMC, Different symbols mark position of stars with short, medium, long and very long periods.

tected eclipsing binary stars should have a counterpart in the neighboring field and compared these objects with actually detected stars. In total, 238 stars should be theoretically paired up. In practice 202 stars with pairs were found, yielding the mean completeness of our catalog equal to about 85%. However it should be noted that this is certainly a lower limit as the regions close to the edge of each field are affected by non-perfect pointing of the telescope leading to effectively smaller number of observations.

Classification types and periods of paired stars were very similar to their counterparts, however we unified them to the values of star with larger number of observations.

Fig. 8 presents the diagram of brightness of the system *vs.*  $\log P$  for stars used in our test. Solid dots mark stars that were paired in the neighboring fields. Crosses show missed pairs. It can be seen that completeness is depending on brightness – most unpaired stars are fainter than  $I \approx 17.5$  mag. Histogram of

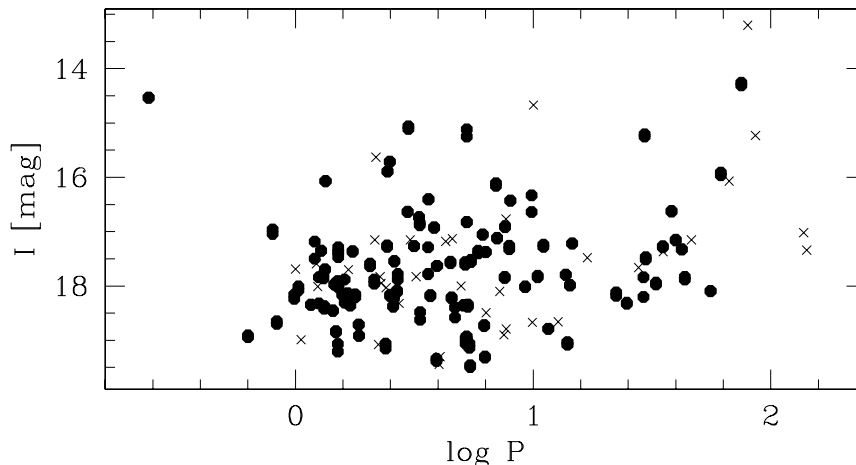


Fig. 8. Diagram of brightness *vs.*  $\log P$  for eclipsing stars which should be paired up with stars located in the neighboring fields. Solid dots mark found paired stars and crosses mark those that remained unpaired.

brightness of all eclipsing binaries (Fig. 3) also indicates, that completeness is likely to be better than 90% for objects brighter than  $I < 17.5$  mag and then it falls gradually to zero for stars fainter than  $I \approx 20$  mag.

We also used paired stars from overlapping fields to check the neural network efficiency. Among 238 stars which should be paired, we found 5 different stars rejected in our pipeline before entering the net, in most cases because of small number of observations. Consequently, only 233 of 238 objects entered the net, leading to only 228 to-be-paired objects. Because we found 202 paired stars, we checked 26 not paired objects and found that 10 of them were rejected by the network (0-class) and one was classified as a “saw-shape” object. Assuming, that the remaining 15 stars (*i.e.*, 6%) passed correctly through the net, but were somehow misclassified or rejected during visual inspection, it gives 217 objects, which were correctly classified by the network. Compared to 228 objects entered, it yields about 95% neural network efficiency. It is worth noticing that the network behavior was “secure” in a sense that it was rather rejecting eclipsing variables than classifying them to wrong classes (one star of 228 gives probability of a mistake less than 1%).

Independently, we checked the network efficiency by visual inspection of all rejected stars (*i.e.*, classified to 0-class) and found additional 146 candidates for eclipsing variables. Compared to 2681 eclipsing stars classified correctly, it yields again about 94% network efficiency. However, one should note, that these tests are only crude approximation and more advanced tests are needed to check neural network efficiency in more detail. Nevertheless, our results are very encouraging and confirm good performance of our algorithm based on artificial neural network. Therefore, it seems it could be applied successfully also in other

implementations of automatic classification of variable stars.

## 7. Candidates for Distance Measurements

Selection of systems suitable for distance determination is one of the main and the most important applications of the catalog of eclipsing binary stars. The catalog contains large number of bright and well detached systems, suitable for spectroscopic study. From EA class, which corresponds to detached eclipsing systems, we selected 36 stars, which satisfied the following criteria: brightness in the  $I$ -band  $< 16$  mag and depth of secondary minimum  $> 0.2$  mag.

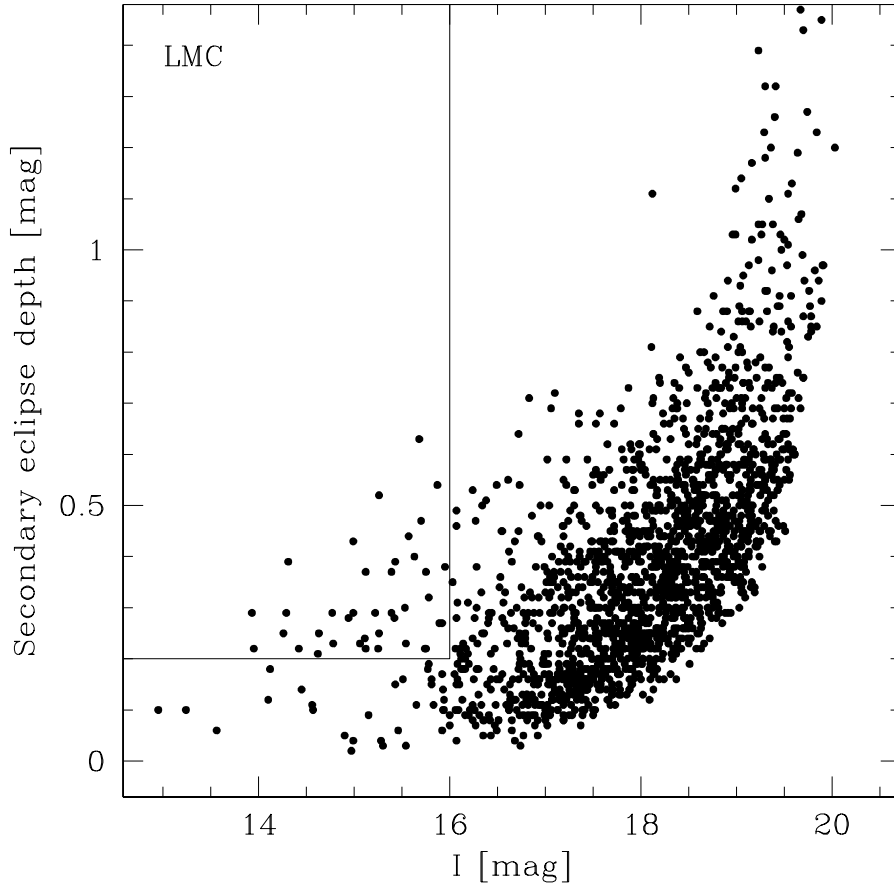


Fig. 9. Depth of the secondary eclipse *vs.*  $I$ -band brightness diagram for EA class of eclipsing binaries detected in the LMC. Lines mark the region with stars that were selected as candidates for distance measurement.



Table 4  
Selected EA eclipsing binary stars suitable for distance measurements to the LMC

No.	Field	Star	Period [days]	$T_0$ −2450000	$I$ (DIA)	$\Delta I_{\text{PRI}}$ (DIA)	$\Delta I_{\text{SEC}}$ (DIA)	$V - I$	$B - V$	Overlap field
112	LMC_SC1	OGLE053459.53-694406.2	75.262000	564.35923	14.31	0.40	0.39	0.00	−0.19	LMC_SC16
114	LMC_SC1	OGLE053502.18-694417.8	2.989580	454.12044	15.11	0.36	0.24	−0.17	−0.18	LMC_SC16
170	LMC_SC2	OGLE053022.67-694126.1	0.645040	455.61994	15.26	0.78	0.25	0.59	0.37	
196	LMC_SC2	OGLE053039.28-701409.7	24.672310	454.56456	14.29	0.31	0.29	0.00	−0.17	
207	LMC_SC2	OGLE053046.88-694759.2	2.917210	453.95612	15.95	1.09	0.38	−0.04	−0.15	
314	LMC_SC2	OGLE053202.60-692717.2	13.267850	458.92109	15.92	0.29	0.27	−0.09	−0.22	
362	LMC_SC2	OGLE053225.29-692537.4	3.370250	456.81334	15.26	0.56	0.52	−0.11	−0.20	
462	LMC_SC3	OGLE052835.52-695102.3	5.638740	457.74472	15.89	1.09	0.27	−0.01	−0.12	
630	LMC_SC4	OGLE052525.66-693304.5	157.554800	380.25443	15.63	0.40	0.30	1.30	1.24	
824	LMC_SC5	OGLE052235.46-693143.4	2.183370	453.36372	15.63	0.43	0.40	−0.17	−0.17	
843	LMC_SC5	OGLE052244.34-693143.5	2.150540	454.36212	15.54	0.27	0.23	−0.16	−0.14	
1129	LMC_SC6	OGLE052100.81-692944.9	1.300790	454.76565	15.42	0.29	0.28	−0.17	−0.15	
1295	LMC_SC7	OGLE051750.09-693827.8	56.234850	448.96592	15.87	0.57	0.54	1.15	1.16	
1321	LMC_SC7	OGLE051804.81-694818.9	3.107040	454.78999	14.77	0.30	0.29	−0.18	−0.16	
1368	LMC_SC7	OGLE051828.18-693745.3	1.403790	455.42725	15.22	0.30	0.29	−0.13	−0.16	
1431	LMC_SC7	OGLE051858.97-693549.5	9.143980	461.16709	15.74	0.34	0.22	−0.15	−0.13	
1450	LMC_SC7	OGLE051911.89-694225.0	2.727130	456.45529	15.43	0.42	0.39	−0.20	−99.99	
1627	LMC_SC8	OGLE051644.53-693233.3	5.603590	457.56235	15.75	0.46	0.37	−0.13	−99.99	
1716	LMC_SC9	OGLE051314.85-691432.5	2.007900	457.58698	13.95	1.58	0.22	0.49	0.33	
1729	LMC_SC9	OGLE051323.98-692249.2	2.636640	456.55989	15.74	0.86	0.82	0.05	0.01	
1748	LMC_SC9	OGLE051341.40-693245.5	5.457280	455.07207	15.53	0.33	0.30	−0.09	−0.12	
1838	LMC_SC10	OGLE051019.64-685812.2	214.379070	390.12764	15.70	0.48	0.47	0.98	0.99	
1849	LMC_SC10	OGLE051028.75-692048.0	3.773360	457.39415	15.78	0.33	0.32	−0.12	−0.15	
1870	LMC_SC10	OGLE051108.69-691216.0	8.000370	455.95671	15.39	0.38	0.37	0.88	0.70	
1967	LMC_SC11	OGLE050828.13-684825.1	2.995410	723.93691	14.63	0.28	0.25	−0.11	−0.16	
1998	LMC_SC11	OGLE050929.29-685502.8	2.678800	727.05172	14.94	0.46	0.28	−0.17	−0.21	
2001	LMC_SC11	OGLE050934.33-685425.9	1.462910	727.75272	15.75	0.23	0.22	−0.10	−0.14	
2157	LMC_SC13	OGLE050634.43-682544.2	2.154480	727.82895	15.12	0.41	0.37	−0.18	−0.17	
2207	LMC_SC14	OGLE050234.59-690546.0	5.255940	725.05728	15.25	0.23	0.22	−0.15	−0.18	LMC_SC15
2321	LMC_SC15	OGLE050140.27-685106.0	4.034850	725.70581	15.39	0.37	0.29	−0.09	−0.13	
2366	LMC_SC16	OGLE053517.75-694318.7	3.881950	729.45995	14.99	0.47	0.43	−0.16	−0.16	
2427	LMC_SC16	OGLE053714.17-702001.5	3.256680	726.33234	15.68	0.66	0.63	−0.07	−0.11	
2456	LMC_SC17	OGLE053818.62-704108.4	2.191320	724.77328	14.42	0.27	0.22	0.10	0.01	
2535	LMC_SC18	OGLE054101.94-700504.7	2.385180	725.42213	15.57	0.47	0.44	0.09	0.02	
2555	LMC_SC18	OGLE054148.68-703531.0	2.768950	726.73270	14.62	0.26	0.21	0.06	−99.99	
2585	LMC_SC19	OGLE054324.89-701650.8	2.054440	725.94139	14.78	0.25	0.23	0.90	0.74	

Fig. 9 presents the diagram of the  $I$ -band brightness *vs.* secondary eclipse depth. The selection region is marked. Note that for a part of objects the depth of the secondary eclipse is deeper than 0.7 mag. For some very ellipsoidal stars this can be a real feature caused by ellipsoidal shape and gravitational darkening. For the others this is probably an artifact caused by crude determination of the depth by automatic procedure in the case of noisy photometry, nonaccurate transformation of the DIA flux differences to magnitudes in the case of blended objects and uncertain period ( $2 \times P$  *vs.*  $P$ ). Table 4 contains main information about the selected stars: number of star in the catalog, field, identification, orbital period, heliocentric J.D. of the primary minimum ( $T_0 - 2450000$ ) corrected for the position of the star in driftscan image,  $I$ -band magnitude,  $I$ -band amplitude (*i.e.*, depth of the primary minimum),  $I$ -band depth of the secondary minimum,  $V - I$  color,  $B - V$  color and overlapping field if a given star is also present. Color value of  $-99.99$  stands for no observations in the  $B$  or  $V$  bands. Appendix D presents the DIA  $I$ -band light curves of 36 selected stars. The ordinate is phase with 0.0 value corresponding to the deeper eclipse. Abscissa is  $I$ -band magnitude. Magnitudes at the top and bottom left are the brightness of the maximum and primary minimum, respectively. Period of the star is also given. Light curve is repeated twice for clarity.

All information about selected eclipsing binaries, light curves as well as finding charts can be found in the OGLE INTERNET archive and *via* WWW Interface (see below).

## 8. The Catalog in the INTERNET

The Catalog of eclipsing binary stars is available on-line through FTP and WWW from the OGLE INTERNET archive. The Catalog can be accessed *via* anonymous FTP at the following addresses:

*ftp://sirius.astroww.edu.pl/~ogle/ogle2/var\_stars/lmc/ecl*  
*ftp://bulge.princeton.edu/~ogle/ogle2/var\_stars/lmc/ecl*

WWW interface to the catalog is available from the following addresses:

*http://www.astroww.edu.pl/~ogle*  
*http://bulge.princeton.edu/~ogle*

The Catalog will be regularly updated when the final set of the OGLE-II data is available and/or any errors, unavoidable in so large dataset, are found. The most recent version will always be available in the INTERNET from the above addresses. The Catalog will also be significantly extended when large enough number of epochs in the ongoing OGLE-III phase is collected. As the OGLE-III fields cover practically entire LMC the final version of the Catalog will include the vast majority of eclipsing stars from the LMC.

## 9. Summary

The catalog of eclipsing binary stars found during the OGLE-II project in the Large Magellanic Cloud is the largest set of such type variable stars. The catalog contains 2580 eclipsing stars of three main types EA, EB and EW. Its high completeness which was obtained by using automated search algorithm based on artificial neural network makes it very useful for many statistical analysis of the LMC stars. Very good quality of photometry and very long time-base of the OGLE-II observations allowed to obtain good quality light curves for most objects in the catalog and very accurate orbital periods. Additionally we selected a subsample of bright detached eclipsing systems suitable for distance determinations. With the high resolution spectra obtained with the largest 6-8 m class telescopes very accurate distance determinations to these objects should be potentially possible, allowing independent, accurate determination of the distance to the LMC.

**Acknowledgements.** We would like to thank Prof. Bohdan Paczyński for his encouragements and discussions about this work. We would also like to thank Dr. Slavek Ruciński for his help, and Dr. Grzegorz Pojmański and Tomasz Mizerski for making their computer programs available. This work was partly supported by the KBN grant 2P03D02523 to L. Wyrzykowski and NASA grant NAG5-12212 and NSF grant AST-0204908 to B. Paczyński. We acknowledge usage of the Digitized Sky Survey which was produced at the Space Telescope Science Institute based on photographic data obtained using the UK Schmidt Telescope, operated by the Royal Observatory Edinburgh.

## REFERENCES

- Alcock, C., *et al.* 1997, *Astron. J.*, **114**, 326.  
 Alcock, C., *et al.* 2002, *Astrophys. J.*, **573**, 338.  
 Akerlof, C., *et al.* 2000, *Astron. J.*, **119**, 1901.  
 Fitzpatrick, E.L., Ribas, I., Guinan, E.F., DeWarf, L.E., Maloney, F.P., and Massa, D. 2002, *Astrophys. J.*, **564**, 260.  
 Grison, P., *et al.* 1995, *Astron. Astrophys. Suppl. Ser.*, **109**, 447.  
 Groenewegen, M.A.T., and Salaris, M. 2001, *Astron. Astrophys.*, **366**, 752.  
 Guinan, E.F., Fitzpatrick, E.L., Dewarf, L.E., Maloney, F.P., Maurone, P.A., Ribas, I., Pritchard, J.D., Bradstreet, D.H., and Giménez, A. 1998, *Astrophys. J. Letters*, **509**, L21.  
 Harries, T.J., Hilditch, R.W., and Howarth, I.D. 2003, *MNRAS*, **339**, 157.  
 Kholopov, P.N., *et al.* 1999, “VizieR On-line Data Catalog”, II/214A.  
 Mizerski, T., and Bejger, M. 2001, *Acta Astron.*, **52**, 61.  
 Nelson, C.A., Cook, K.H., Popowski, P., and Alves, D.R. 2000, *Astron. J.*, **119**, 1205.  
 Paczyński, B. 1997, in: “The Extragalactic Distance Scale STScI Symposium”, Baltimore, Cambridge University Press, p. 273 (astro-ph/9608094).  
 Pojmański, G. 2002, *Acta Astron.*, **52**, 397.  
 Ribas, I., Fitzpatrick, E.L., Maloney, F.P., Guinan, E.F., and Udalski, A. 2002, *Astrophys. J.*, **574**, 771.  
 Ruciński, S. 1993, *P.A.S.P.*, **105**, 1433.  
 Ruciński, S. 1997, *Astron. J.*, **113**, 1112.  
 Schwarzenberg-Czerny, A. 1989, *MNRAS*, **241**, 153.

- Soszyński, I., Żebruń, K., Udalski, A., Woźniak, P.R., Szymański, M., Kubiak, M., Pietrzyński, G., Szewczyk, O., and Wyrzykowski, L. 2002, *Acta Astron.*, **52**, 143.
- Szymański, M., Kubiak, M., and Udalski, A. 2001, *Acta Astron.*, **51**, 259.
- Udalski, A., Olech, A., Szymański, M., Kałużny, J., Kubiak, M., Mateo, M., Krzemiński, W., and Stanek, K.Z. 1997a, *Acta Astron.*, **47**, 1.
- Udalski, A., Kubiak, M., and Szymański, M. 1997b, *Acta Astron.*, **47**, 319.
- Udalski, A., Szymański, M., Kubiak, M., Pietrzyński, G., Woźniak, P.R., and Żebruń, K. 1998a, *Acta Astron.*, **48**, 147.
- Udalski, A., Pietrzyński, G., Woźniak, P.R., Szymański, M., Kubiak, M., and Żebruń, K. 1998b, *Astrophys. J. Letters*, **509**, L25.
- Udalski, A., Soszyński, I., Szymański, M., Kubiak, M., Pietrzyński, G., Woźniak, P.R., and Żebruń, K. 1999, *Acta Astron.*, **49**, 223.
- Udalski, A., Szymański, M., Kubiak, M., Pietrzyński, G., Soszynski, I., Woźniak, P., and Żebruń, K. 2000, *Acta Astron.*, **50**, 307.
- Woźniak, P.R. 2000, *Acta Astron.*, **50**, 421.
- Woźniak, P.R., *et al.* 2001, *Astron. Astrophys. Suppl. Ser.*, **199**, 130.04.
- Żebruń, K., Soszyński, I., and Woźniak, P.R. 2001a, *Acta Astron.*, **51**, 303.
- Żebruń, K., Soszyński, I., Woźniak, P.R., Udalski, A., Kubiak, M., and Szymański, M., Pietrzyński, G., Szewczyk, O., and Wyrzykowski, L. 2001b, *Acta Astron.*, **51**, 317.

## **Appendix A**

**Eclipsing stars in the LMC**

**EA type eclipsing stars**

see OGLE INTERNET Archive

## **Appendix B**

**Eclipsing stars in the LMC**

**EB type eclipsing stars**

see OGLE INTERNET Archive

## **Appendix C**

**Eclipsing stars in the LMC**

**EW type eclipsing stars**

see OGLE INTERNET Archive

## **Appendix D**

**Eclipsing stars in the LMC**

**Selected detached eclipsing stars**

files: AppD.1.jpg, AppD.2.jpg

This figure "AppD.1.jpg" is available in "jpg" format from:

<http://arxiv.org/ps/astro-ph/0304458v1>

This figure "AppD.2.jpg" is available in "jpg" format from:

<http://arxiv.org/ps/astro-ph/0304458v1>

This figure "fig2.jpg" is available in "jpg" format from:

<http://arxiv.org/ps/astro-ph/0304458v1>



This figure "fig4.jpg" is available in "jpg" format from:

<http://arxiv.org/ps/astro-ph/0304458v1>

This figure "fig6.jpg" is available in "jpg" format from:

<http://arxiv.org/ps/astro-ph/0304458v1>